



Francisella tularensis Uses Cholesterol and Clathrin-Based Endocytic Mechanisms to Invade Hepatocytes

H. T. Law^{1*}, Ann En-Ju Lin^{1*}, Youra Kim¹, Brian Quach¹, Francis E. Nano² & Julian Andrew Guttman¹

¹Simon Fraser University Department of Biological Sciences Shrum Science Centre Room B8276 Burnaby, BC, V5A 1S6, ²University of Victoria Department of Biochemistry and Microbiology Victoria, BC, V8W 3P6.

SUBJECT AREAS:
PATHOGENS
IMAGING
CELLULAR MICROBIOLOGY
BIOLOGICAL MODELS

Received
23 August 2011

Accepted
28 November 2011

Published
14 December 2011

Correspondence and requests for materials should be addressed to J.A.G. (jguttman@sfu.ca)

* These authors contributed equally to this work.

Francisella tularensis are highly infectious microbes that cause the disease tularemia. Although much of the bacterial burden is carried in non-phagocytic cells, the strategies these pathogens use to invade these cells remains elusive. To examine these mechanisms we developed two *in vitro* *Francisella*-based infection models that recapitulate the non-phagocytic cell infections seen in livers of infected mice. Using these models we found that *Francisella novicida* exploit clathrin and cholesterol dependent mechanisms to gain entry into hepatocytes. We also found that the clathrin accessory proteins AP-2 and Eps15 co-localized with invading *Francisella novicida* as well as the *Francisella* Live Vaccine Strain (LVS) during hepatocyte infections. Interestingly, caveolin, a protein involved in the invasion of *Francisella* in phagocytic cells, was not required for non-phagocytic cell infections. These results demonstrate a novel endocytic mechanism adopted by *Francisella* and highlight the divergence in strategies these pathogens utilize between non-phagocytic and phagocytic cell invasion.

The potentially fatal disease tularemia is caused by the pathogenic microbe *Francisella tularensis* subspecies *tularensis* (*F. tularensis*). These bacteria are highly virulent as exposure to as few as 10 organisms can result in 30–35% mortality if left untreated¹. *F. tularensis* enter hosts through a variety of routes including inhalation, ingestion, abrasion and transmission through arthropod vectors. Within their hosts these microbes colonize a variety of organs including the lungs, spleen, and liver^{2,3}. *F. tularensis* encode a secretion system that shares homology with type VI secretion gene clusters, as well as crucial genes needed for intracellular growth and virulence on a region of their bacterial chromosome called the *Francisella* Pathogenicity Island^{4,5}. Much of the work examining the genetics, biochemistry and cell biology of *F. tularensis* exploit two closely related surrogate *F. tularensis* subspecies: *Francisella tularensis* subspecies *novicida* (*F. novicida*); a murine pathogen that does not normally cause disease in healthy humans⁶ but colonizes identical organs as *F. tularensis* during *in vivo* murine infections⁷ and infects both phagocytic⁴ and non-phagocytic cells^{6,8–10}. *F. novicida* and *F. tularensis* share >97% of their DNA sequence⁶ and both have homologous virulence factors. The second surrogate commonly used is *F. tularensis* subspecies *holarctica* Live Vaccine Strain (*Francisella* LVS); an attenuated strain that can infect human and murine cells^{8,9,11}.

Microbes often utilize multiple strategies to gain entry into cells. The process of endocytosis encompasses both the internalization of extracellular particles into phagocytic cells [by phagocytosis] and non-phagocytic cells [referred to as pinocytosis]¹². These entry methods center around the use of the large GTPase, dynamin II, in releasing the endocytic vesicles from the invaginating membrane at the final stage of endocytosis (scission). Dynamin dependent pinocytosis is sub-divided into two categories; clathrin-mediated or caveolin-mediated pinocytosis¹². Clathrin-mediated pinocytosis uses the coat protein clathrin and a number of accessory proteins to create a structure known as a clathrin-coated vesicle (CCV) for internalization. Although the mechanism of pinocytosis was thought to be restricted to the internalization of vesicles ranging from 30 nm to 150 nm in diameter, recent work has demonstrated that bacteria and ligand coated beads up to 5.5 μ m are readily internalized into cells via clathrin-mediated endocytosis¹³. Caveolin-mediated endocytosis utilizes caveolin-1, a cholesterol-binding integral membrane protein, to form 50–80 nm flask-shaped membrane invaginations called caveolae. Caveolae are also associated with sphingolipid and cholesterol-rich sub-domains, commonly called lipid rafts¹⁴. Consequently, perturbation of cholesterol or lipid rafts often impede caveolin-dependent endocytosis¹⁵. Dynamin-independent pinocytosis has emerged as an internalization strategy utilized by many microbes^{16–18}.



This type of pinocytosis can be separated into three general divisions: 1) non-clathrin/non-caveolin dependent pinocytosis, 2) macropinocytosis, and 3) lipid raft-mediated pinocytosis¹⁴.

Like many invasive pathogens, *F. tularensis* gain entry into host cells as an initial step of infection. Efficient internalization of *F. tularensis* in macrophages has been shown to require complement¹⁹. Additionally, through the use of the cholesterol sequestering agent Methyl- β -cyclodextran in combination with a plasma membrane marker, it has been suggested that cholesterol-rich microdomains of the plasma membrane, also known as lipid rafts²⁰ are also involved in *F. tularensis* internalization into phagocytes^{20,21}. These factors together with the endocytic protein caveolin-1 are thought to synergistically participate in the invasion of *Francisella* in phagocytic cells²⁰. Although *Francisella* has been known to invade non-phagocytic cells^{8–10}, the mechanism of *Francisella* entry into these types of cells has not yet been elucidated. In order to examine the sub-cellular mechanisms *Francisella* use to invade hepatocytes, we developed two *F. novicida* infection models using two different non-phagocytic murine hepatocyte cell lines, NMuLi and BNL CL.2 cells. Through the coupling of our *in vitro* systems with pharmacological inhibitors and RNA interference (RNAi), we demonstrate that the

clathrin-associated machinery together with cholesterol are vital for efficient *F. novicida* invasion into non-phagocytic cells, and that this internalization is independent of caveolin.

Results

Murine hepatocytes, a target of *F. novicida*. *F. tularensis* are known to infect both phagocytic^{22–25} and non-phagocytic host cells^{9,11,26}; however studies examining non-phagocytic epithelial cells during these infections have trailed those of phagocytes. In order to generate a baseline for comparison we initially examined *F. novicida* infections occurring within murine hepatocytes by using the common *F. novicida* infection strategy of intraperitoneally infecting mice with ~ 50 *F. novicida*^{27,28}. At 48 h post-infection, livers were collected from mice and subsequently co-stained with anti-albumin antibodies, a classical marker of hepatocytes^{29–31} and anti-*F. novicida* antibodies. Cells that stained positive for albumin were typically infected in clusters, and varied from a few bacteria within a single cell to an unmeasurable number of *F. novicida* that completely filled the host cytoplasm (Figure 1A). By using microscopy and manually enumerating cells infected with *F. novicida* in liver cross sections, we found that 11.3% of albumin-positive cells and 1.1% of albumin-negative cells (those that did not react with anti-albumin antibodies) were infected (Figure 1B). This work thus sets a benchmark for the establishment of our epithelial cell culture models using *F. novicida* and suggested that the majority of infected cells within the livers of *F. novicida* infected mice were hepatocytes.

To generate cell culture models that would be useful for studying *F. novicida* hepatocyte infections, we selected two non-phagocytic hepatocyte cell lines, BNL CL.2 and NMuLi cells. We confirmed their hepatocyte characteristic by immunolocalizing albumin in those cell lines and found that both cell lines contained the classical albumin staining present in hepatocytes (Figure S1). Following that verification, both cell types were infected at a multiplicity of infection (MOI) of 100 for 24 h. During these infections the number of intracellular bacteria varied from <10 , to hundreds of bacteria within the cytosol of a single cell (Figure 2A). Approximately 15.8% of BNL CL.2 and 25.4% of NMuLi cells became infected with *F. novicida* (Figure 2B) and the bacterial clustering patterns observed *in vivo* were also evident in the *in vitro* results (Figure 1A, 2A). Next, we examined the colonization levels of *F. novicida* during shorter infection durations and coupled microscopic examinations with invasion assays using both cell lines. We found a modest level of invasion at 4 h and 8 h ($\sim 10^4$ CFU/mL), whereas the highest level of intracellular bacteria were detected at 24 h of infection (10^6 CFU/mL) (Figure 2A), suggesting that the bacteria had invaded the hepatocytes and likely replicated within them.

Francisella enters non-phagocytes through a clathrin and cholesterol-dependent mechanism.

Diverse endocytic strategies are used by microbes to gain entry into non-phagocytic cells³². To evaluate the internalization mechanism(s) that promote *F. novicida* invasion of hepatocytes, we used invasion assays together with pharmacological inhibitors that disrupt specific cellular components to block particular endocytic functions. Clathrin-mediated endocytosis (CME) is a classical pathway often used by pathogens to gain entry into non-phagocytic cells (extensively reviewed by others³³ and our lab³²). To determine whether CME was involved in *F. novicida* invasion, we analyzed levels of bacterial internalization in the presence of the chemical inhibitors monodansylcadaverine (MDC) and chlorpromazine (CPZ), which are frequently used to study the role of CME during pathogen invasion^{34,35}. MDC is a transglutaminase inhibitor that prevents the assembly of clathrin-coated pits (CCP) at the plasma membrane, whereas CPZ functions as a clathrin-sequestering agent, inhibiting endosomal recycling of clathrin. We pre-treated both NMuLi and BNL CL.2 cells with CPZ

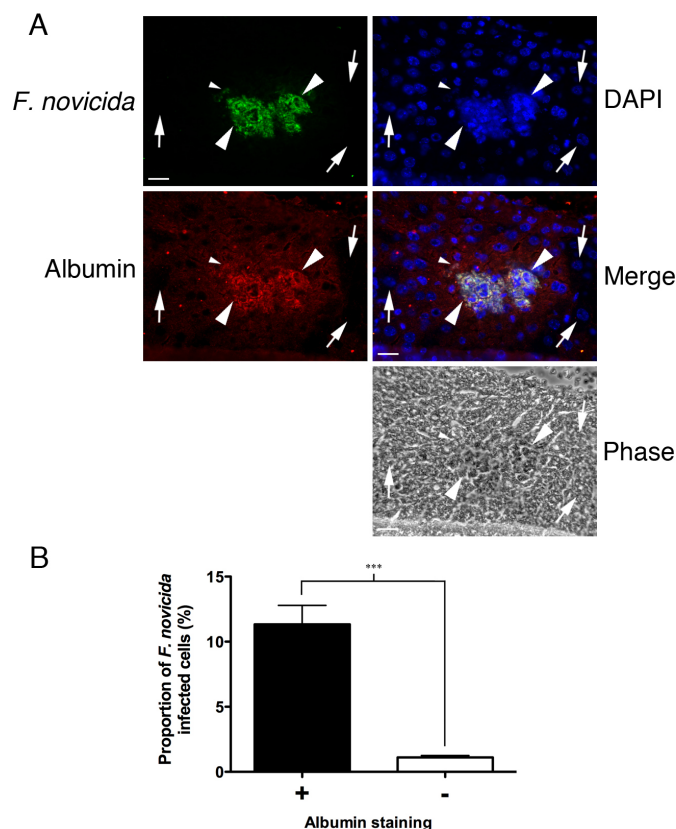


Figure 1 | *F. novicida* colonization of murine hepatocytes. (A) Immunofluorescent and phase micrographs showing wild-type *F. novicida*, albumin, and DNA [DAPI] localization in infected liver tissue section harvested from mice challenged via the intraperitoneal route. Arrows indicate uninfected albumin-negative cells, large arrowheads point to infected albumin-positive cells containing uncountable levels of *F. novicida* and the small arrowhead points to an albumin-positive cells with few internalized bacteria respectively. Scale bar = 10 μ m. (B) Quantification of cells infected with *F. novicida* based on immunofluorescent images of tissue sections stained with anti-mouse albumin and anti *F. novicida* antibodies. n (below) is defined as the number of tissue section regions collected in which image stacks were taken (each image stack represents between 500 to 1500 cells). Mouse 1 (n=17), Mouse 2 (n=21), and Mouse 3 (n=17). *** P<0.0001.

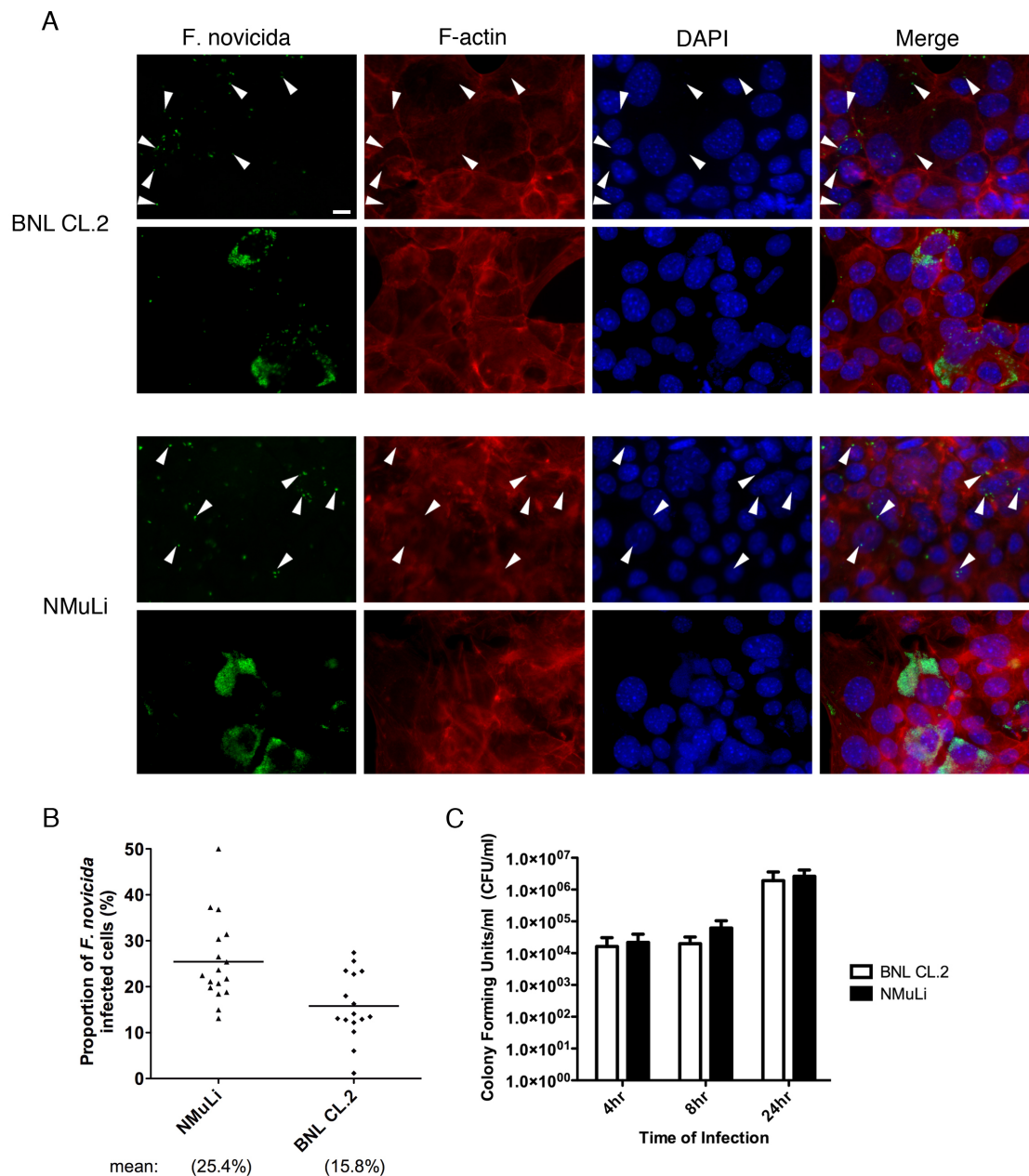


Figure 2 | *F. novicida* invades and replicates within BNL CL.2 and NMuLi hepatocytes. (A) Immunofluorescent images of *F. novicida* infections in cultured hepatocytes. Hepatocytes were fixed following 24 h *F. novicida* infections with both BNL CL.2 and NMuLi cells. Samples were labelled with anti-*F. novicida* antibodies (green), fluorescent phalloidin [to indicate the cell boundaries] (red) and DAPI (blue). Arrowheads indicate some of the bacteria within the infected cells. Scale bar = 10 μ m. (B) Quantification of the proportion of infected hepatocytes as assessed by microscopic examination. NMuLi (n=17) and BNL CL.2 (n=16). (C) Titre of intracellular *F. novicida* at various timepoints following infection of BNL CL.2 and NMuLi cell infections by invasion assay (n=3).

and MDC at various concentrations for 30 minutes prior to infections with *F. novicida* and analyzed their effects on bacterial invasion. *F. novicida* internalization into host cells was reduced at 80 μ M MDC (by ~60%) and 5 μ M CPZ (by 40–50%) as compared to untreated cells (Figures 3A, 4A). Neither condition caused any detectable cytotoxicity to host cells or bacteriocidal effects as drug treated cells remained morphologically viable and intact when observed by phase contrast microscopy (data not shown). Because these drugs are well-known inhibitors that are specific for blocking CME, the loss of bacterial invasion in drug treated cells suggested that *F. novicida* invasion likely occurred through a CME pathway.

Despite the presence of the CME blocking agents, *F. novicida* still exhibited the ability to enter epithelial cells (Figure 3A, 4A), suggesting that *F. novicida* likely use alternative route(s) in addition to CME

for entry. To investigate how *F. novicida* could invade epithelial cells with dysfunctional clathrin machinery, we examined clathrin-independent endocytic mechanisms, such as caveolin and lipid-raft dependent endocytosis, both of which require cholesterol-rich domains^{36,37}. Extraction of cholesterol from the plasma membrane using methyl- β -cyclodextrin (M β CD), a potent inhibitor that disrupts lipid composition and thus cholesterol-based endocytosis^{20,38}, caused a statistically significant reduction, of ~60%, in *F. novicida* invasion (Figure 3B, 4B). We performed additional tests using a combination of progesterone (a cholesterol-synthesis inhibitor) and nystatin (a cholesterol-sequestering agent) [Prog/Nys] to validate the importance of lipid raft domains during these invasion events. Interruption of synthesis and transport of cholesterol to membrane lipid-raft domains by these drugs caused a moderate

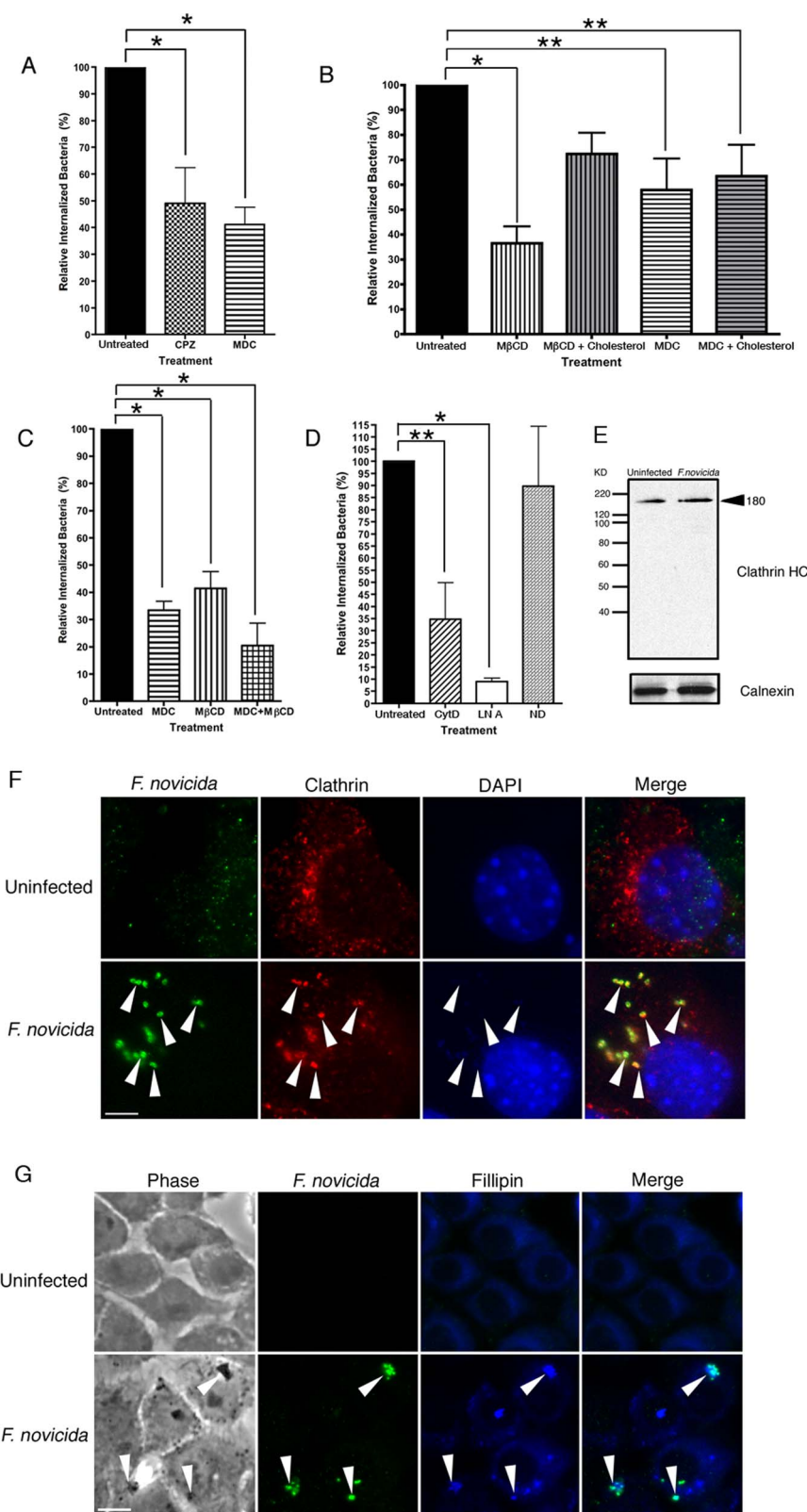


Figure 3 | Internalization of *F. novicida* into BNL CL.2 cells is a clathrin- and cholesterol-dependent process that requires actin. (A–D) BNL CL.2 cells were pre-treated with the indicated drugs and incubated with *F. novicida* for 22 h followed by a 2 h gentamicin treatment for CFU enumeration. (A) Clathrin inhibitors: 80 μ M monodansylcadaverine (MDC) or 5.0 μ M chlorpromazine (CPZ). (B) Cholesterol inhibitors: 2.5 mM M β CD or 80 μ M MDC supplemented with 1 mM cholesterol. (C) Individual or a combination of 2.5 mM M β CD and 80 μ M MDC. (D) Cytoskeleton inhibitors: 5 μ M cytochalasin D (CytD), 2.5 μ M latrunculin A (LN A) or 2.5 μ M nocardazole (ND), * $P < 0.01$. ** $P < 0.05$. (E) Western blot shows that the overall level of clathrin heavy-chain (HC) protein remains unaltered after 24 h *F. novicida* infections of BNL CL.2 cells compared to uninfected cells. For immunolocalization experiments, untreated cells were infected with *F. novicida* for 8 h, fixed and stained with (F) an anti-*F. novicida* antibody (green), anti-clathrin HC (red) and DAPI or (G) an anti-*F. novicida* antibody (green) and filipin (blue) as well as phase contrast. Arrowheads indicate some of the bacteria that co-localize with the other labels. Scale bar = 5 μ m.

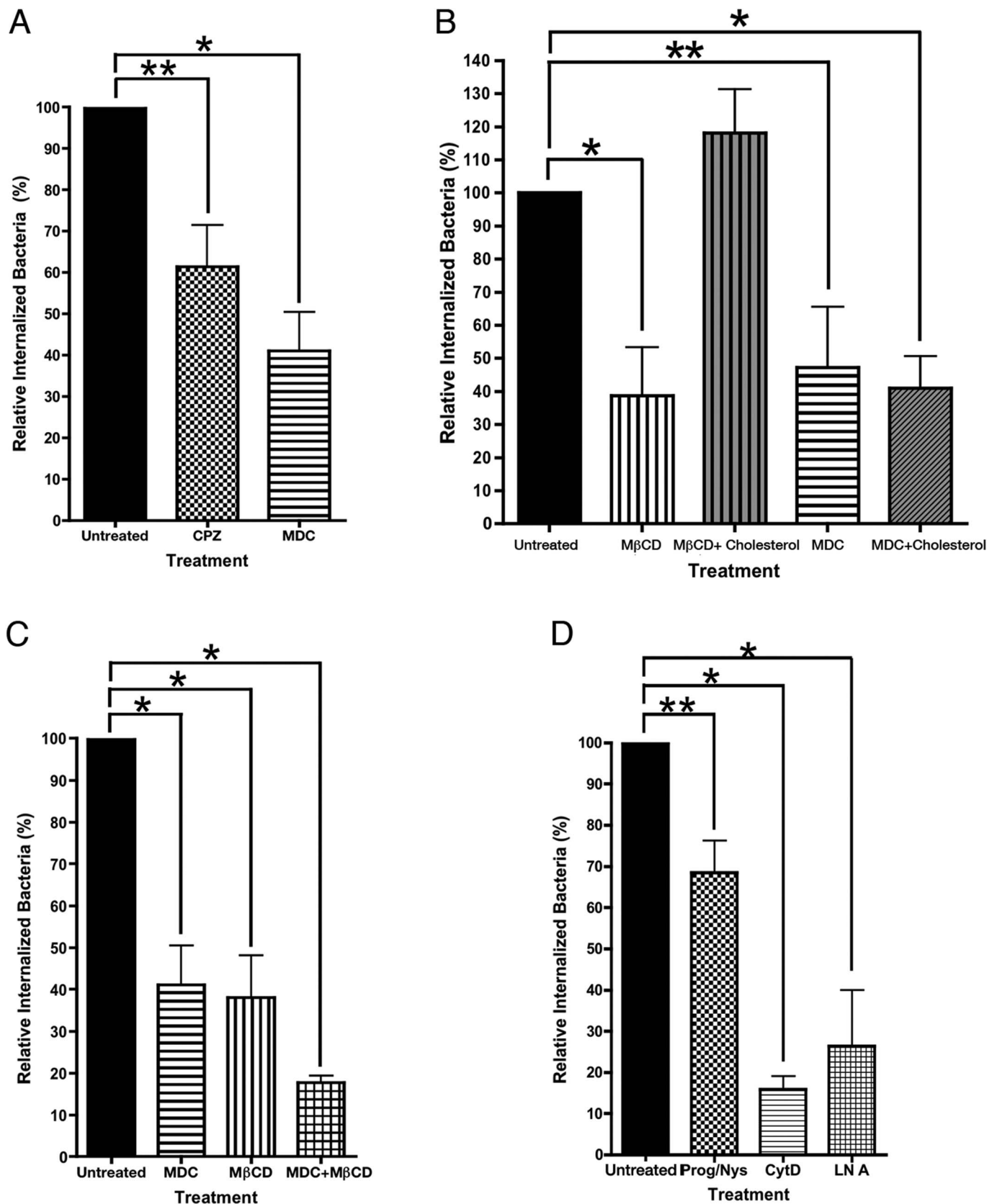


Figure 4 | Internalization of *F. novicida* into NMuLi cells is a clathrin- and cholesterol dependent process that requires actin. NMuLi cells were pre-treated with the indicated drugs and incubated with *F. novicida* for 22 h followed by a 2 h gentamicin treatment for CFU enumeration. (A) Clathrin inhibitors: 80 μ M monodansylcadaverine (MDC) or 5.0 μ M chlorpromazine (CPZ). (B) Cholesterol inhibitors: 2.5 mM M β CD or 80 μ M MDC supplemented with 1 mM cholesterol. (C) Individual or combination of 2.5 mM M β CD and 80 μ M MDC. (D) Cells were treated simultaneously with 2 μ g/mL progesterone and 10 μ M nystatin (Prog/Nys). Cytoskeleton inhibitors: 5 μ M cytochalasin D (CytD), 2.5 μ M latrunculin A (LN A) * $P < 0.01$, ** $P < 0.05$.



(~30%), yet statistically significant inhibition in *F. novicida* uptake in epithelial cells (Figure 4D). This data suggests that the presence of cholesterol at the plasma membrane is necessary for efficient invasion given that removal of cholesterol caused more prominent defects in invasion as compared to lipid-raft disruption through cholesterol binding. The importance of cholesterol at the plasma membrane for *F. novicida* invasion was further emphasized when the invasion levels were almost restored to those of untreated cells when cells that were pre-treated with M β CD were supplemented with excess cholesterol prior to the infections (Figure 3B). By contrast, replacement of cholesterol failed to enhance *F. novicida* invasion in MDC treated cells. To further analyze the importance of cholesterol and CME during *F. novicida* invasion, a combination of M β CD and MDC were used concurrently to deplete both cholesterol and clathrin in host cells, thus blocking both CME and cholesterol-dependent endocytosis. This further exaggerated the inhibitory effect of *F. novicida* internalization when compared to a single inhibitor treatment, as the invasion level was diminished by ~80% (Figure 3C). We also explored other possible endocytic pathways such as caveolin-dependent endocytosis and/or macropinocytosis that might be used by *F. novicida*. To accomplish this, we infected cells in the presence of filipin, a cholesterol-sequestering agent that impairs the membrane invagination of caveolae and consequently prevents caveolin-based endocytosis³⁷. *F. novicida* invasion appeared to be resistant to filipin treatment as it did not significantly impede invasion levels in either BNL CL.2 or NMuLi hepatocytes (Figure 5A). Further analysis by immunolocalization also revealed a normal pattern of caveolin at the cell periphery and within the cytoplasm that resembled untreated cells; the cytoplasmic caveolin did not accumulate near *F. novicida* throughout different stages of infection [at 8 h, 16 h or 24 h post-infection] (Figure 5B). These results strongly indicate that caveolin likely does not participate in *F. novicida* invasion of hepatocytes. To assess whether *F. novicida* engages in macropinocytosis during invasion, we examined cellular invasion in the presence of amiloride, an inhibitor of the Na⁺/H⁺ exchange channel at the plasma membrane known to specifically block internalization via macropinocytosis³⁹. Treatment with amiloride did not cause any notable changes in *F. novicida* invasion, especially when compared to *Salmonella* Typhimurium invasion, which uses well established macropinocytosis strategies to invade their host's cells (Figure 5C)^{40,41}. This result is consistent with the lack of actin membrane ruffles (a characteristic of macropinocytosis) in the vicinity of *F. novicida* during the invasion process (Figure 2A), thus strengthening the evidence that *F. novicida* does not utilize macropinocytosis during its invasion process of hepatocytes.

Having demonstrated that clathrin and cholesterol inhibitors significantly attenuate *F. novicida* invasion, we extended our study by immunolocalizing clathrin and cholesterol to assess whether they became re-distributed during this process. To visualize clathrin localization during invasion, BNL CL.2 cells were infected with *F. novicida* for 8 h and co-localized with anti-*F. novicida* and anti-clathrin antibodies. We chose the 8 h timepoint in an attempt to identify regions of bacterial invasion without significant cytoplasmic bacterial replication so that the precise localization of the proteins could be identified at sites of bacterial contact. We found that while the overall protein levels of clathrin remained unchanged (Figure 3F), clathrin localized strongly at sites where *F. novicida* interacted with the host cells (Figure 3E). This finding was also evident in BNL CL.2 cells during *Francisella* LVS invasion as clathrin was found to associate closely with invading *Francisella* LVS following 8 h infections (Figure S2). To examine the distribution of cholesterol, we took advantage of the cholesterol binding property of the fluorescent probe filipin^{36,42}. Similar to clathrin staining, we observed an accumulation of filipin at sites of *F. novicida* invasion (Figure 3F). Altogether, our data suggest that *F. novicida* invades epithelial cells at cholesterol-rich domains, in a clathrin-dependent manner.

Clathrin accessory proteins Eps15 and AP-2 are recruited and required for efficient *Francisella* invasion. To investigate whether *F. novicida* utilize the protein assembly of classical-CME machinery for cell invasion, we examined the roles of CME adaptor proteins during *F. novicida* invasion of non-phagocytic cells. Using a similar approach as aforementioned, we immunolocalized Eps15 and AP-2 (housekeeping components that typically participate in cargo recognition and CCP formation to facilitate the progression of CME⁴³) 8 hours post-infection and found that both Eps15 and AP-2 were recruited to sites of invasion and co-localized with *F. novicida* in a similar pattern as was found with clathrin (Figure 6A, 6D). Identical results were also found during *Francisella* LVS infections as bacteria were co-localized with cellular Eps15 and AP-2 after 8 h infections (Figure S2). Eps15 or AP-2 protein expression levels remained unchanged in cells infected with *F. novicida* when compared to uninfected cells (Figure 6B, 6E). Because both AP-2 and Eps15 are major constituents of CCPs and govern the progression of CME, recruitment of these molecules to sites of *Francisella* interaction with host cells strongly supports the notion that *Francisella* exploit CME as a route for epithelial cell entry.

We continued our study by investigating the importance of Eps15 and AP-2 in *F. novicida* invasion. Using RNAi, we knocked down both Eps15 and AP-2 (α -adaplin subunit) to undetectable levels (Figure 6B, 6E). Depletion of these proteins have been shown to impede CME of many extracellular cargos, including microbes⁴⁴. We found that loss of Eps15 caused a significant inhibition in clathrin-dependent internalization of *F. novicida*, resulting in only ~20% invasion relative to cells treated with non-targeting control pool (CP) siRNA (Figure 6C). To confirm the importance of clathrin-coat formation at the plasma membrane during the invasion process, we knocked down AP-2, which is known to cause an interruption in CCP assembly. Consistent with results from Eps15 RNAi, AP-2 depleted cells also exhibited a significant decrease in *F. novicida* invasion, with ~40% of invasion remaining when compared to untreated cells (Figure 6F). Collectively, these data show that the clathrin adaptors AP-2 and Eps15 are essential for clathrin-dependent uptake of *F. novicida*.

Disruption of actin polymerization interferes *F. novicida* internalization. The cytoskeleton is known to be an integral element necessary for functional and efficient endocytosis^{45,46}. Using the cytoskeletal targeting drugs, cytochalasin-D (Cyt D) and colchicines, Craven and co-workers had previously demonstrated that both actin filaments and microtubules were used by *Francisella* LVS to efficiently invade pulmonary epithelial cells⁸. To assess whether *F. novicida* required these filament systems for efficient invasion in hepatocytes, we utilized the cytoskeletal inhibitors Cyt D and latrunculin A (LN A) to block actin filament polymerization. Additionally, we used nocodazole, a pharmacological drug that interferes with microtubule polymerization. Consistent with a previous *Francisella* LVS report in alveolar epithelial cells⁴⁷, we found that cells pre-treated with the actin-disrupting agents exhibited a significant defect in *F. novicida* invasion in hepatocytes. Cells pre-treated with Cyt D or LN A blocked >60% of bacterial entry as compared to untreated cells (Figure 3D, 4D). In contrast, nocodazole treated cells did not exhibit any significant defects in internalizing *F. novicida* (Figure 3D). Together, these results suggest that the actin machinery, but not microtubules, is needed for efficient *F. novicida* invasion into hepatocytes. To further delineate the role of actin during *F. novicida* invasion, we immunolocalized actin filaments at 8 h and 24 h of infection and detected no direct association of actin and *F. novicida* at either time point (Figure 2). Consequently, it appears that *F. novicida* either uses actin for invasion via an indirect manner or could use it as part of the CME process, as the actin cytoskeleton has been described to play an important role in facilitating CME⁴⁶.

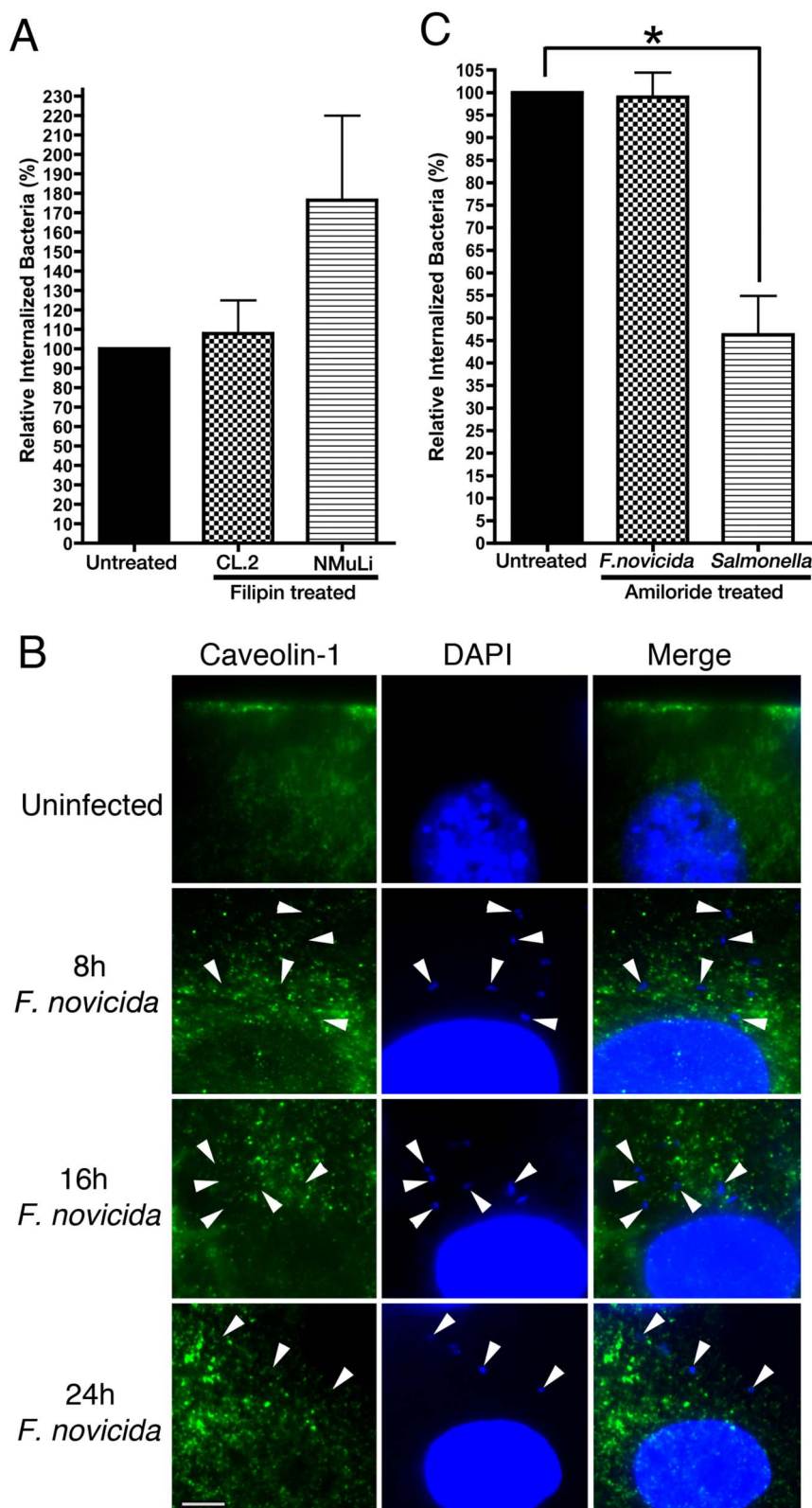


Figure 5 | *F. novicida* entry does not utilize caveolin-dependent or macropinocytosis pathways. (A) BNL CL.2 and NMuLi cells were treated with the caveolin-inhibitor filipin and infected with *F. novicida* for 22 h followed by 2 h gentamicin treatment for invasion assays. (B) Immunolocalization of caveolin-1 (green) and DAPI (blue) of uninfected BNL CL.2 cells or following 8 h, 16 h, and 24 h infections with *F. novicida* showed no co-localization between *F. novicida* and caveolin-1. Arrowheads indicate the localization of *F. novicida*. Scale bar=5 μ m. (C) 5 mM of amiloride was used to pre-treat BNL CL.2 cells and HeLa cells for 15 min prior to infection with *F. novicida* and *Salmonella* Typhimurium (SL1344), respectively. Untreated cells were treated with media containing DMSO. Cells infected with *F. novicida* for 6 h followed by 2 h gentamicin treatment did not show a decrease in invasion while cells infected with *S. Typhimurium* for 30 min followed by 1 h gentamicin treatment showed a significant decrease in invasion * $P < 0.01$.

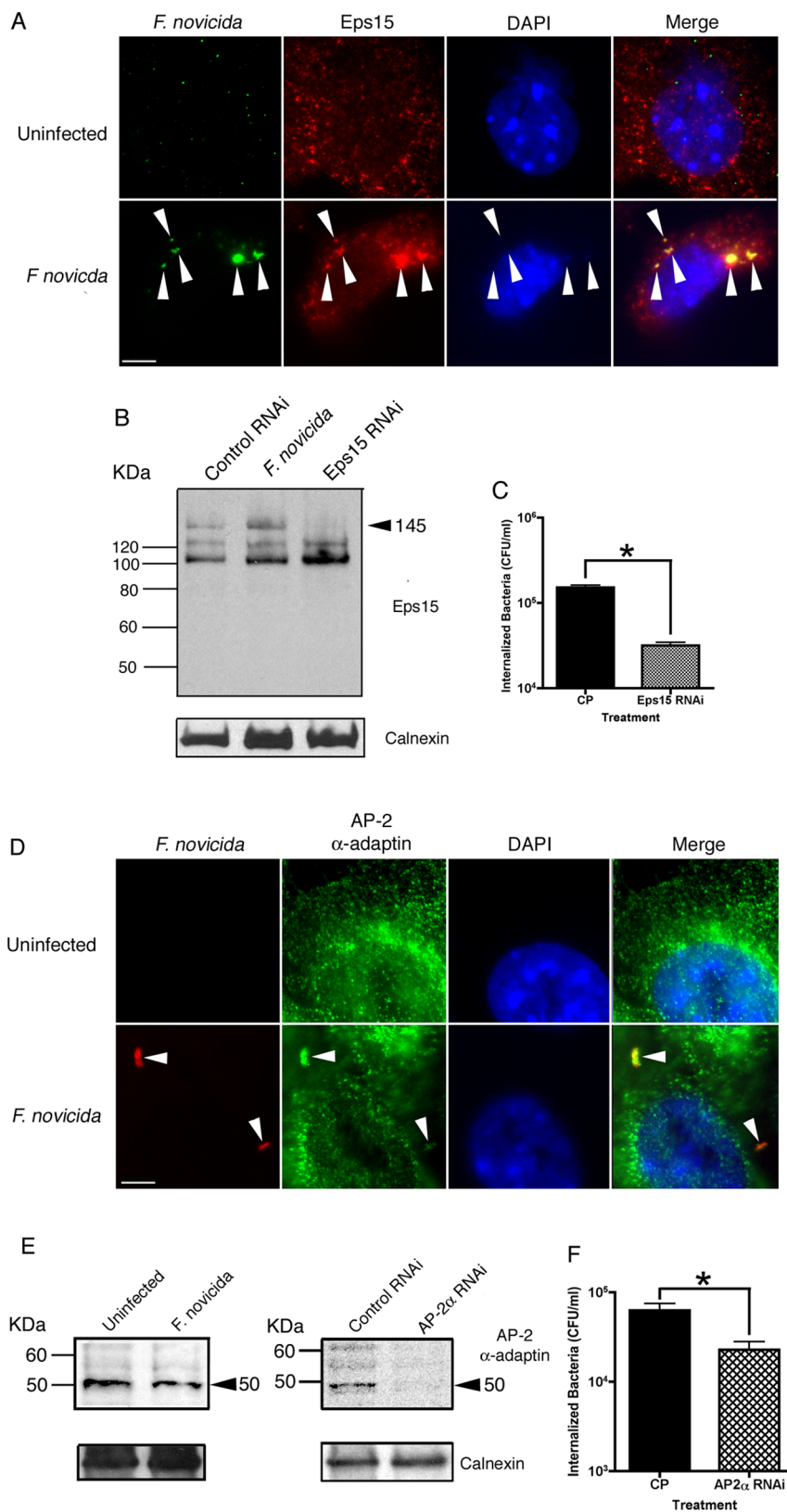


Figure 6 | Clathrin-associated adaptor proteins Esp15 and AP-2 are crucial for *F. novicida* invasion into non-phagocytic cells. (A, D) BNL CL.2 cells were infected with *F. novicida* for 8 h and immunolocalized with anti-*F. novicida* together with (A) anti-Eps15 (red) or (D) anti-AP-2 α -adaptin (green) antibodies. Arrowheads indicate bacteria and protein co-localization. Scale bar = 5 μ m. (B and E). Western blots show the overall protein levels of (B) Eps15 (145 kDa) or (E) AP-2 α -adaptin (50 kDa) in 8 h *F. novicida* infected cells (untreated with RNAi) remained unchanged compared to uninfected control. Cells transiently transfected with siRNA (48 h) showed a significant reduction in the targeted Eps15 or AP-2 α -adaptin proteins as compared to cells transfected with siRNA control pool (CP). (C and F) Reduced Eps15 and AP-2 α -adaptin lead to a significant defect in *F. novicida* internalization 24 h post-infection. * $P < 0.05$.



Discussion

Over the past number of years a familiar theme of endocytic protein hijacking by microbial pathogens has developed. Although *Francisella* has been identified as an invasive intracellular pathogen^{2,3}, a general lack of knowledge of its internalization process and lifestyle in non-phagocytic cells remains. Most of the previous *Francisella* invasion studies into non-phagocytic cells have been focused on examinations of the *Francisella* live vaccine strain (LVS). One study demonstrated that the *Francisella* LVS can invade and replicate within murine alveolar cells *in vivo*, as well as in TC-1 and MLE 12 murine lung epithelial cell lines and human alveolar type2 cells A549⁸. Another study demonstrated that the *Francisella* LVS can infect Hep-2 and human bronchial epithelial [HBE] cells *in vitro*; invasion assays showed relatively low levels of *Francisella* LVS invasion in these cells 5 hours post-infection, as approximately 5×10^3 – 10^4 CFU were recovered, representing 0.05%–0.1% of the initial inoculum⁴⁷. Although these important studies demonstrated the ability of *Francisella* LVS to replicate within these cell types, the internalization strategies utilized by these microbes during their invasion events still required further investigation. Because of the fastidious nature of the *Francisella* LVS, we opted to primarily use *F. novicida* as a model of *F. tularensis* infections. Using these bacteria we demonstrated a high level of colonization in murine hepatocyte *in vivo* and to elucidate their mechanisms of entry we developed 2 robust *in vitro* hepatocyte infection models.

We initiated our study by utilizing a panel of drugs that target specific endocytic pathways; none of the drugs used in the study caused adverse effects in bacterial growth, which suggested that the inhibitory effects we observed specifically impeded bacterial entry instead of bacterial replication. Although centrifugation of bacteria onto the host cells is a strategy that some laboratories use to enhance host cell contact with the microbes, in our experiments we allowed the bacteria to attach and colonize onto the surface of host cells without external forces to decrease the external influences during the infections. After monitoring levels of *F. novicida* infection in the hepatocytes throughout a 24 h period, we found a moderate degree of bacterial containment within the hepatocytes at the 8 h time point and not surprisingly a much higher level of invasion 24 h post-infection. Unlike many fast-invading bacteria such as *Salmonella* Typhimurium, which invade within 30 minutes⁴⁰, *F. novicida* required an extended amount of time to initiate invasion into host cells for suitable detection and analysis. As a result, we chose to primarily monitor *F. novicida* invasion for up to 24 h infections to have ample numbers of internalized bacteria for comparison. Extended infection durations are not uncommon, as *Helicobacter pylori* invasion into cultured cells occurs at 24 h post-infection⁴⁸ and *Chlamydia trachomatis* invasion is often assessed between 24 h to 72 h post-infection^{49,50}. Using MDC and CPZ, we first found that the loss of functional CME caused a significant decrease in *F. novicida* invasion when assessed at 24 h. Furthermore, we identified clathrin and major associated proteins at the *Francisella* entry sites after 8 h of infection. Taken together, these results suggest that CME is a key pathway targeted by these microbes, regardless of the endpoint assayed.

CME is a complex and multi-step process that involves many clathrin accessory proteins to complete the process. Among the ~20 accessory proteins, Eps15 and AP-2 have been shown to be important for efficient internalization of molecules in general⁵¹. Our finding of impaired *F. novicida* invasion following Eps15 and AP-2 siRNA treatment highlights the importance of these clathrin-mediated endocytic proteins and CME as a whole during *Francisella* invasion.

Because *F. novicida* retained some capacity to invade these epithelial cell lines in the absence of functional CME, we postulated that another strategy must also be involved. Using the strong cholesterol-binding agent M β CD we extracted cholesterol from the membrane

and found a significant decrease in *F. novicida* uptake. This phenotype reverted when the samples were supplemented with excess cholesterol. These findings coupled with the observation of cholesterol at *F. novicida* entry sites is reminiscent of cholesterol recruitment seen during *Shigella flexneri* invasion of HeLa cells⁴².

Because phagocytic cells have been shown to use caveolin during *F. novicida* invasion events, we also studied its involvement and found that caveolin was not required for hepatocyte invasion, despite our findings that invasion requires cholesterol. Such dependence on cholesterol-rich domains in the absence of caveolin is not exclusive to *F. novicida* as it has been previously demonstrated during the invasion of viral (i.e., Simian virus 40)⁵² bacterial (i.e., *Brucella abortus*)⁵³, as well as a much larger parasitic (*Toxoplasma gondii*)⁵⁴ pathogens.

Recruitment of actin filaments at the site of internalization has been recognized as important processes during endocytosis, as polymerization of actin creates mechanical force to promote membrane curvature and invagination⁵⁵. In this study, we have shown that *F. novicida* invasion is severely inhibited in the presence of the actin inhibitor cytochalasin D without detecting any notable membrane ruffling as seen during *Salmonella* invasion; similar results were previously described in a *Francisella* LVS invasion study using HEp-2 cells⁴⁷ and murine alveolar cells TC-1⁸. While it is likely that *F. novicida* invasion does not induce massive actin reorganization at the invasion sites, it has also been challenging to detect the small amounts of actin recruited to sites of endocytosis using fluorescent microscopy. Based on the involvement of actin in endocytosis^{46,55}, we suspect that the inhibition of invasion through the impairment of the actin cytoskeleton likely comes from the association of the actin meshwork and endocytic events⁴⁶. While the same *Francisella* LVS studies also suggested *Francisella* entry into TC-1 lung epithelial cells and human HEp-2 epithelial cells required microtubule^{8,47}, we did not detect any notable defects in *F. novicida* invasion into either NMuLi or BNL.CL2 cells when infected with *F. novicida* in the presence of the microtubule disrupting drug nocodazol. This discrepancy could be due to the difference in the *Francisella* strain and host cell types used.

Collectively, we have demonstrated *F. novicida* uses multiple strategies for efficient internalization into hepatocytes, which involves functional clathrin-mediated endocytosis and cholesterol-rich microdomains.

Methods

Bacteria and growth conditions. *F. tularensis* subsp. *novicida* strain U112 was grown on trypticase soy agar (TSA) or broth (TSB) supplemented with 0.1% L-cysteine at 37°C. The bacteria were grown to stationary phase for 18 h at 37°C with shaking at 220 rpm. *Salmonella* Typhimurium (strain SL1344) was grown using the same parameters on Luria Bertani (LB) agar or broth.

Animal infections, tissue preparation and tissue immunolocalization. Female BALB/C mice aged 6–8 weeks (Charles River Laboratories, Quebec, Canada) were left undisturbed to recover from transport for at least 4 days. Infections were performed by intraperitoneal injection of 50 ± 10 *F. novicida* bacteria in 100 μ l of TSB + 0.1% L-cysteine. Immediately following the infection, the identical volumes of the bacterial culture were spread onto TSA-C plates. Colony forming units (CFUs) were enumerated after plates were incubated overnight at 37°C. Following 48 h infections, mice were euthanized and livers extracted then submerged into 3% paraformaldehyde (room temperature) in phosphate-buffered saline (PBS; 150 mM NaCl, 5 mM KCl, 0.8 mM KH₂PO₄, 3.2 mM Na₂HPO₄, pH 7.3) for 3 h. After 3 successive 10 min PBS washes, fixed organs were frozen (using liquid nitrogen) and attached to an aluminum stub by OCT compound (Sakura Finetek USA, Torrance). 5 μ m frozen sections were cut and attached to Superfrost (VWR) glass slides that were pre-coated with 0.01% poly-L-lysine solution (Sigma). Slides with attached tissue sections were immediately plunged into –20°C acetone for 5 min, air-dried, then blocked with 5% “Blotto” non-fat dry milk (Santa Cruz Biotechnology) in PBS for 20 min. The slides were then incubated overnight at 4°C with a 1 : 1000 dilution of rabbit anti-*F. novicida* antibodies^{4,56} and 20 ng/ μ l goat anti-mouse albumin (Bethyl Laboratories Inc.) antibodies diluted in PBS containing 1% Tween-20 and 1% non-fat milk. The following day the sections were washed 3 times for 10 min each with TPBS/non-fat milk (1% Tween-20 and 0.1% non-fat milk in PBS) before being incubated for 2 h with 20 ng/ μ l Alexa Fluor 594 donkey anti-goat antibodies (Invitrogen) then with 20 ng/ μ l Alexa Fluor 488 goat anti-rabbit antibodies for 1 h (Invitrogen). After the last set of washes, coverslips were mounted using Prolong Gold (Invitrogen). Images



were acquired using a Leica DMI4000B inverted fluorescent microscope equipped with a Hamamatsu Orca R2 CCD camera (Hamamatsu, Japan) and Metamorph Imaging System software (Universal Imaging Corp., Pennsylvania). The presence of albumin in cells was assessed by examining samples and those that did not react were considered absent of albumin. In all of those instances positively reacting cells were also present in the samples, which acted as positive controls for the experiment. For antibody specificity controls, primary antibodies were replaced with normal immunoglobulin from the host animal species at identical concentrations to the primary antibodies.

Cell lines and culture model infection parameters. Cultured BNL CL.2 (TIB-73) and NMuLi (CRL-1638) murine hepatocytes (ATCC) were grown in high-glucose Dulbecco's modified Eagle's medium (DMEM) (Thermo Scientific) supplemented with 10% Fetal Bovine Serum (FBS) at 37°C and 5% CO₂. Cells were grown to confluence in 6- or 24-well cell culture plates overnight in 10% FBS in DMEM before switching to 10% FBS in DMEM supplemented with 0.1% L-cysteine prior to infection.

Cultured cell invasion assays and inhibitor studies. Inhibitors targeting different endocytic pathways were used to evaluate levels of *F. novicida* invasion. The duration of treatments and concentrations were determined and optimized according to previous studies as well as cell viability assays. BNL CL.2 or NMuLi cells were seeded at a concentration of $\sim 1.5 \times 10^5$ cells/mL in 24-well culture plates and used 24 h after seeding. Monolayers of confluent cells were pre-incubated at 37°C with the following inhibitors for 30 min: 5 μ M chlorpromazine, 5 μ M cytochalasin D, 2.5 μ M lantruculin A, 2.5 mM M β CD, 80 μ M MDC, 2 μ g/mL progesterone combined with 10 μ M nystatin. Cells were pre-treated for 2 h with 2.5 μ M nocodazole and 15 min with 5 mM amiloride at 37°C prior to infection. For the cholesterol supplementation study, 1 mM solubilized cholesterol in chloroform was added to M β CD treated cells at a final concentration of 2 mM for 30 min prior to infection. All compounds (purchased from Sigma) were maintained in the media during infections except amiloride, which was removed prior to infections. Untreated controls are only treated with carrier buffer (ie: DMSO) in the absence of inhibitors. Following pre-treatment, cells were infected with *F. novicida* at an MOI of 100. At 22 h post-infection, cells were washed three times with warm DMEM + 10% FBS and treated with media containing 100 μ g/ml gentamicin for 2 h at 37°C to kill extracellular bacteria. For amiloride studies, cells were infected with *F. novicida* at an MOI of 100 for 6 h followed by 2 h gentamicin treatment. As a positive control, HeLa cells were infected with *Salmonella* Typhimurium at an MOI of 100 for 30 min followed by 1 h gentamicin treatment. After 3 PBS washes, cells were lysed either mechanically using a 27^{1/2} gauge needle or chemically using 1% Triton X-100 in PBS. The released internalized bacteria were immediately serially diluted and plated on TSA-C for colony-forming unit (CFU) enumeration to quantify levels of internalization.

Cultured cell immunolocalization. Cells were grown to $\sim 80\%$ confluency on sterile No.1.5 glass coverslips in 6-well culture plates. Prior to infection, media was replaced with DMEM + 10% FBS with 0.1% cysteine. After 8 h, 16 h or 24 h infections at an MOI of 100, cells were fixed in 3% paraformaldehyde in PBS for 15 min, washed three times with PBS, incubated with 0.2% Triton X-100 and treated with 5% NGS following chemical reagent or antibody treatments in processes mentioned above. Cholesterol localization was determined using a UV fluorescent cholesterol binding fungal toxin, filipin, which binds cholesterol and emits blue fluorescence. Cells were incubated with filipin (50 μ g/mL) for 30 min at RT, washed three times with PBS, then co-localized with *F. novicida*. Clathrin, Eps15, AP-2 and caveolin-1 localization was performed using mouse anti-clathrin heavy chain antibodies at 15.6 μ g/ml (BD Biosciences), mouse anti-Eps15 (clone 17) antibodies at 16.67 μ g/ml (Santa Cruz Biotechnology), mouse anti-AP2 α -adaptin (3B5) at 10 μ g/ml (BD Biosciences), or mouse anti-caveolin-1 (clone 2297) antibodies at 16.67 μ g/ml (BD Biosciences). Prior to staining with clathrin, Eps15 and AP-2 antibodies, the antibodies were pre-cleared against *F. novicida* to ensure no cross reactivity with the bacteria. To accomplish this, 1 ml of live *F. novicida* was pelleted, fixed for 20 min with 500 μ l of 3% paraformaldehyde in PBS at RT then washed 6 times with PBS at 15 min intervals. *F. novicida* was pelleted and re-suspended overnight at 4°C with the antibody, prepared at the concentrations described above, then used for immunolocalization.

Cell lysate preparation and western blotting. BNL CL.2 cells were grown on 150 mm tissue culture dishes and infected at an MOI ~ 100 with *F. novicida* for 24 h. Cells were washed 3 times with PBS containing 1 mM CaCl₂ and 1 mM MgCl₂ followed by treatment with RIPA lysis buffer (150 mM NaCl, 50 mM Tris pH 7.4, 5 mM EDTA, 1% Nonidet P-40, 1% Deoxycholic acid, 10% SDS) for 10 min on ice. Western blotting was performed according to Guttman and colleagues⁵⁷. Briefly, equal amounts of total protein was loaded and separated on 10% SDS-polyacrylamide gels and transferred to nitrocellulose membranes (Bio-Rad Laboratories). Membranes were blocked with 5% non-fat milk and washed in Tris-buffered saline with 0.1% Tween-20 (TBST) 3 times for 5 min. A primary rabbit anti-Eps15 antibody (Santa Cruz Biotechnology, CA) was used at 1.0 μ g/ml, a mouse anti-AP2 α -adaptin (3B5) antibody (Trevor Williams lab, Developmental Studies Hybridoma Bank, IA) was used at 0.725 μ g/ml, and a mouse anti-clathrin heavy chain antibody (BD Biosciences) was used at 0.25 μ g/ml. Antibodies were prepared in TBST supplemented with 1% BSA. After washing, a horseradish peroxidase (HRP)-conjugated secondary antibody (Cell Signaling Technology) was used as previously

described⁵⁷. Signals were detected by enhanced chemiluminescence (Perkin Elmer) and exposed on Kodak BioMax light film.

RNA interference. Small interfering RNA (siRNA) ON-TARGETplus SMART pools were synthesized and purchased from Dharmacon, targeting Eps15 (Catalog: 004005) and AP-2 A1 α -adaptin (Catalog: 11771). For RNAi controls, equal amount of siGENOME Non-Targeting siRNA Pool (Catalog: D-001206-13) was used. BNL CL.2 cells were grown in 24 well plates to 40% confluency and transfected with 50 nM of the siRNA pool using the jetPRIME transfection reagent or INTERFERin (Polyplus transfection) according to the manufacturer's procedures. At 48 h post-transfection, cells were either treated with RIPA lysis buffer supplemented with a protease inhibitor cocktail (Roche) for cell lysates, or infected with *F. novicida* for 24 h before being processed for invasion assays.

Statistical analysis. All experiments were performed at least in triplicate during a single run, and repeated a minimum of three times. For enumerating infected murine liver cells, phase and fluorescent images of liver cells stained for albumin (or F-actin), *F. novicida*, and DNA were overlaid and tallied using Fiji software (<http://fiji.sc/wiki/index.php/Fiji>). Localization of *F. novicida* within the cytoplasm of albumin-positive and negative cells were considered 'infected', whereas cells that show no *F. novicida* localization within the cell periphery were counted as 'uninfected'. Each field of view was acquired as a stack under both phase-contrast and fluorescent microscopy. Student's *t*-test was applied to determine statistical significance between the two experimental groups. For inhibitor studies, results were expressed as the means \pm standard deviation (s.d.) from repeated independent experiments. Differences between untreated and inhibitor treated samples were compared using One-way ANOVA followed by Dunnett's Multiple Comparison Test ($P < 0.05$). Differences between control pool and RNAi treatments were compared using Student's *t* test. ($P < 0.05$).

- Ellis, J., Oyston, P. C., Green, M. & Titball, R. W. Tularemia. *Clin Microbiol Rev* **15**, 631–646 (2002).
- Conlan, J. W., Chen, W., Shen, H., Webb, A. & KuoLee, R. Experimental tularemia in mice challenged by aerosol or intradermally with virulent strains of Francisella tularensis: bacteriologic and histopathologic studies. *Microb Pathog* **34**, 239–248 (2003).
- Conlan, J. W. & North, R. J. Roles of Listeria monocytogenes virulence factors in survival: virulence factors distinct from listeriolysin are needed for the organism to survive an early neutrophil-mediated host defense mechanism. *Infect Immun* **60**, 951–957 (1992).
- Schmerk, C. L., Duplantis, B. N., Howard, P. L. & Nano, F. E. A Francisella novicida pdpA mutant exhibits limited intracellular replication and remains associated with the lysosomal marker LAMP-1. *Microbiology* **155**, 1498–1504 (2009).
- Qin, A. & Mann, B. J. Identification of transposon insertion mutants of Francisella tularensis tularensis strain Schu S4 deficient in intracellular replication in the hepatic cell line HepG2. *BMC Microbiol* **6**, 69 (2006).
- Sentic, M., Al-Khodor, S. & Abu Kwaik, Y. Cell biology and molecular ecology of Francisella tularensis. *Cell Microbiol* **12**, 129–139.
- Ojeda, S. S. *et al.* Rapid dissemination of Francisella tularensis and the effect of route of infection. *BMC Microbiol* **8**, 215 (2008).
- Craven, R. R., Hall, J. D., Fuller, J. R., Taft-Benz, S. & Kawula, T. H. Francisella tularensis invasion of lung epithelial cells. *Infect Immun* **76**, 2833–2842 (2008).
- Melillo, A. *et al.* Identification of a Francisella tularensis LVS outer membrane protein that confers adherence to A549 human lung cells. *FEMS Microbiol Lett* **263**, 102–108 (2006).
- Mortensen, B. L. *et al.* Effects of the putative transcriptional regulator IclR on Francisella tularensis pathogenesis. *Infect Immun* **78**, 5022–5032 (2010).
- Hall, J. D. *et al.* Infected-host-cell repertoire and cellular response in the lung following inhalation of Francisella tularensis Schu S4, LVS, or U112. *Infect Immun* **76**, 5843–5852 (2008).
- Doherty, G. J. & McMahon, H. T. Mechanisms of endocytosis. *Annu Rev Biochem* **78**, 857–902 (2009).
- Veiga, E. *et al.* Invasive and adherent bacterial pathogens co-Opt host clathrin for infection. *Cell Host Microbe* **2**, 340–351 (2007).
- Lajoie, P. & Nabi, I. R. Regulation of raft-dependent endocytosis. *J Cell Mol Med* **11**, 644–653 (2007).
- Thomas, C. M. & Smart, E. J. Caveolae structure and function. *J Cell Mol Med* **12**, 796–809 (2008).
- Saeed, M. F., Kolokoltsov, A. A., Albrecht, T. & Davey, R. A. Cellular entry of ebola virus involves uptake by a macropinosytosis-like mechanism and subsequent trafficking through early and late endosomes. *PLoS Pathog* **6**, (2010).
- Vidricaire, G. & Tremblay, M. J. A clathrin, caveolae, and dynamin-independent endocytic pathway requiring free membrane cholesterol drives HIV-1 internalization and infection in polarized trophoblastic cells. *J Mol Biol* **368**, 1267–1283 (2007).
- Furuta, N. *et al.* Porphyromonas gingivalis outer membrane vesicles enter human epithelial cells via an endocytic pathway and are sorted to lysosomal compartments. *Infect Immun* **77**, 4187–4196 (2009).



19. Clemens, D. L., Lee, B. Y. & Horwitz, M. A. Francisella tularensis enters macrophages via a novel process involving pseudopod loops. *Infect Immun* **73**, 5892–5902 (2005).
20. Tamilselvam, B. & Daefler, S. Francisella targets cholesterol-rich host cell membrane domains for entry into macrophages. *J Immunol* **180**, 8262–8271 (2008).
21. Barel, M. *et al.* A novel receptor-ligand pathway for entry of Francisella tularensis in monocyte-like THP-1 cells: interaction between surface nucleolin and bacterial elongation factor Tu. *BMC Microbiol* **8**, 145 (2008).
22. Anthony, L. D., Burke, R. D. & Nano, F. E. Growth of Francisella spp. in rodent macrophages. *Infect Immun* **59**, 3291–3296 (1991).
23. Santic, M., Molmeret, M., Klose, K. E. & Abu Kwaik, Y. Francisella tularensis travels a novel, twisted road within macrophages. *Trends Microbiol* **14**, 37–44 (2006).
24. Oyston, P. C., Sjøstedt, A. & Titball, R. W. Tularemia: bioterrorism defence renews interest in Francisella tularensis. *Nat Rev Microbiol* **2**, 967–978 (2004).
25. Geier, H. & Celli, J. Phagocytic receptors dictate phagosomal escape and intracellular proliferation of Francisella tularensis. *Infect Immun* **79**, 2204–2214 (2011).
26. Ludu, J. S. *et al.* The Francisella pathogenicity island protein PdpD is required for full virulence and associates with homologues of the type VI secretion system. *J Bacteriol* **190**, 4584–4595 (2008).
27. Kieffer, T. L., Cowley, S., Nano, F. E. & Elkins, K. L. Francisella novicida LPS has greater immunobiological activity in mice than F. tularensis LPS, and contributes to F. novicida murine pathogenesis. *Microbes Infect* **5**, 397–403 (2003).
28. Tempel, R., Lai, X. H., Crosa, L., Kozlowicz, B. & Heffron, F. Attenuated Francisella novicida transposon mutants protect mice against wild-type challenge. *Infect Immun* **74**, 5095–5105 (2006).
29. Shanmukhappa, K., Mourya, R., Sabla, G. E., Degen, J. L. & Bezerra, J. A. Hepatic to pancreatic switch defines a role for hemostatic factors in cellular plasticity in mice. *Proc Natl Acad Sci U S A*, **102**, (2005).
30. Haozui, D. *et al.* Three-dimensional polarization sensitizes hepatocytes to Fas/CD95 apoptotic signalling. *J Cell Sci* **118**, 2763–2773 (2005).
31. Tanimizu, N., Saito, H., Mostov, K. & Miyajima, A. Long-term culture of hepatic progenitors derived from mouse Dlk+ hepatoblasts. *J Cell Sci* **117**, 6425–6434 (2004).
32. Lin, A. E. & Guttman, J. A. Hijacking the endocytic machinery by microbial pathogens. *Protoplasma*, **244**, 75–90 (2010).
33. Pizarro-Cerda, J., Bonazzi, M. & Cossart, P. Clathrin-mediated endocytosis: what works for small, also works for big. *Bioessays*, **32**, 496–504 (2010).
34. Boisvert, H. & Duncan, M. J. Clathrin-dependent entry of a gingipain adhesin peptide and Porphyromonas gingivalis into host cells. *Cell Microbiol* **10**, 2538–2552 (2008).
35. Acosta, E. G., Castilla, V. & Damonte, E. B. Alternative infectious entry pathways for dengue virus serotypes into mammalian cells. *Cell Microbiol* **11**, 1533–1549 (2009).
36. Lafont, F. & van der Goot, F. G. Bacterial invasion via lipid rafts. *Cell Microbiol* **7**, 613–620 (2005).
37. Fielding, C. J. & Fielding, P. E. Relationship between cholesterol trafficking and signaling in rafts and caveolae. *Biochim Biophys Acta* **1610**, 219–228 (2003).
38. Shin, J. S., Gao, Z. & Abraham, S. N. Involvement of cellular caveolae in bacterial entry into mast cells. *Science*, **289**, 785–788 (2000).
39. Koivusalo, M. *et al.* Amiloride inhibits macropinocytosis by lowering submembranous pH and preventing Rac1 and Cdc42 signaling. *J Cell Biol* **188**, 547–563.
40. Chen, L. M., Hobbie, S. & Galan, J. E. Requirement of CDC42 for Salmonella-induced cytoskeletal and nuclear responses. *Science*, **274**, 2115–2118 (1996).
41. Francis, C. L., Ryan, T. A., Jones, B. D., Smith, S. J. & Falkow, S. Ruffles induced by Salmonella and other stimuli direct macropinocytosis of bacteria. *Nature*, **364**, 639–642 (1993).
42. Lafont, F., Tran Van Nhieu, G., Hanada, K., Sansonetti, P. & van der Goot, F. G. Initial steps of Shigella infection depend on the cholesterol/sphingolipid raft-mediated CD44-IpaB interaction. *EMBO J* **21**, 4449–4457 (2002).
43. Traub, L. M. Tickets to ride: selecting cargo for clathrin-regulated internalization. *Nat Rev Mol Cell Biol* **10**, 583–596 (2009).
44. Cureton, D. K., Massol, R. H., Saffarian, S., Kirchhausen, T. L. & Whelan, S. P. Vesicular stomatitis virus enters cells through vesicles incompletely coated with clathrin that depend upon actin for internalization. *PLoS Pathog* **5** (2009).
45. Samaj, J. *et al.* Endocytosis, actin cytoskeleton, and signaling. *Plant Physiol* **135**, 1150–1161 (2004).
46. Collins, A., Warrington, A., Taylor, K. A. & Svitkina, T. Structural organization of the actin cytoskeleton at sites of clathrin-mediated endocytosis. *Curr Biol* **21**, 1167–1175 (2011).
47. Lindemann, S. R., McLendon, M. K., Apicella, M. A. & Jones, B. D. An in vitro model system used to study adherence and invasion of Francisella tularensis live vaccine strain in nonphagocytic cells. *Infect Immun* **75**, 3178–3182 (2007).
48. Oliveira, M. J. *et al.* Helicobacter pylori induces gastric epithelial cell invasion in a c-Met and type IV secretion system-dependent manner. *J Biol Chem* **281**, 34888–34896 (2006).
49. Hybiske, K. & Stephens, R. S. Mechanisms of Chlamydia trachomatis entry into nonphagocytic cells. *Infect Immun* **75**, 3925–3934 (2007).
50. Stuart, E. S., Webley, W. C. & Norkin, L. C. Lipid rafts, caveolae, caveolin-1, and entry by Chlamydiae into host cells. *Exp Cell Res* **287**, 67–78 (2003).
51. Traub, L. M. & Lukacs, G. L. Decoding ubiquitin sorting signals for clathrin-dependent endocytosis by CLASPs. *J Cell Sci* **120**, 543–553 (2007).
52. Damm, E. M. *et al.* Clathrin- and caveolin-1-independent endocytosis: entry of simian virus 40 into cells devoid of caveolae. *J Cell Biol* **168**, 477–488 (2005).
53. Watarai, M., Makino, S., Fujii, Y., Okamoto, K. & Shirahata, T. Modulation of Brucella-induced macropinocytosis by lipid rafts mediates intracellular replication. *Cell Microbiol* **4**, 341–355 (2002).
54. Coppens, I. & Joiner, K. A. Host but not parasite cholesterol controls Toxoplasma cell entry by modulating organelle discharge. *Mol Biol Cell* **14**, 3804–3820 (2003).
55. Kaksonen, M., Toret, C. P. & Drubin, D. G. Harnessing actin dynamics for clathrin-mediated endocytosis. *Nat Rev Mol Cell Biol* **7**, 404–414 (2006).
56. Nano, F. E. Identification of a heat-modifiable protein of Francisella tularensis and molecular cloning of the encoding gene. *Microb Pathog* **5**, 109–119 (1988).
57. Guttman, J. A. *et al.* Aquaporins contribute to diarrhoea caused by attaching and effacing bacterial pathogens. *Cell Microbiol* **9**, 131–141 (2007).

Acknowledgement

We would like to thank Karen Lo for her technical assistance. JAG is a CIHR New Investigator. AEL is funded through a CIHR CGS and the MSFHR. Funding was provided through operating grants from CIHR and NSERC. The authors declare no conflicts of interest in connection with the manuscript.

Author contributions

HTL and AEL performed the experiments, analyzed the results and wrote the manuscript. HTL prepared figures 1–2; AEL prepared figures 3–6; YK contributed to figure 3 and 4; BQ contributed to figure 1; FEN participated in data analysis and reviewed the manuscript; JAG participated in data analysis and wrote the manuscript.

Additional information

Supplementary information accompanies this paper at <http://www.nature.com/scientificreports>

Competing financial interests: The authors declare no competing financial interests.

License: This work is licensed under a Creative Commons Attribution-NonCommercial-ShareAlike 3.0 Unported License. To view a copy of this license, visit <http://creativecommons.org/licenses/by-nc-sa/3.0/>

How to cite this article: Law, H.T. *et al.* Francisella tularensis uses cholesterol and clathrin-based endocytic mechanisms to invade hepatocytes. *Sci. Rep.* **1**, 192; DOI:10.1038/srep00192 (2011).